Applied Materials Today xxx (xxxx) xxx

Contents lists available at ScienceDirect

Applied Materials Today

journal homepage: www.elsevier.com/locate/apmt

2D siloxene sheets: A novel electrochemical sensor for selective dopamine detection

Rajendran Ramachandran[a,b,c], Xiaohui Leng[b], Changhui Zhao[b], Zong-Xiang Xu[c,**], Fei Wang[b,d,*]

[a] SUSTech Academy for Advanced Interdisciplinary Studies, Southern University of Science and Technology, Shenzhen 518055, China
[b] School of Microelectronics, Southern University of Science and Technology, Shenzhen 518055, China
[c] Department of Chemistry, Southern University of Science and Technology, Shenzhen 518055, China
[d] GaN Device Engineering Technology Research Center of Guangdong, Southern University of Science and Technology, Shenzhen 518055, China

ARTICLE INFO

Article history:
Received 8 July 2019
Received in revised form 6 September 2019
Accepted 29 September 2019

Keywords:
Siloxene
Dopamine
Electrochemical sensor
Differential pulse voltammetry

ABSTRACT

In this work, a novel electrochemical sensor based on siloxene material is proposed for selective detection of dopamine (DA). We have prepared a two-dimensional silicon material called siloxene sheets via deintercalation of calcium from calcium disilicide ($CaSi_2$) and reviewed their electrocatalytic activity towards DA sensing. Characterization methods like X-ray diffraction, scanning electron microspore, transmission electron microscope, X-ray photoelectron spectroscopy, and Brunauer–Emmett–Teller surface analyser were employed for analysing the material properties of the as-prepared siloxene. Electrochemical tests proved that the siloxene modified glassy-carbon electrode (siloxene/GCE) exhibited the excellent activity of dopamine detection. The fabricated electrode demonstrated a low detection limit of 0.327 μM with a wide linear range (10–190 μM; 200–1100 μM). The proposed sensor also showed excellent selectivity, stability, and reusability. This work suggests that the electrodes with siloxene based materials are promising for electrochemical sensors application.

1. Introduction

Two-dimensional (2D) nanomaterials have acquired significant research attention in the modern world [1,2]. Since the advent of the graphene material, the research directions turned into finding new 2D materials for potential applications [3,4]. Up to date, numerous 2D materials including transition metal dichalcogenides (TMDs) like molybdenum diselenide ($MoSe_2$) [5], molybdenum disulphide (MoS_2) [6], as well as phosphorene [7], graphitic carbon nitride (g-C_3N_4) [8], MXene materials [9] have been discovered and developed for various applications, especially for electrochemical applications such as energy conversion and storage like supercapacitors, batteries, hydrogen evaluation and electrochemical biosensors [10–14]. The investigation of the electrochemistry of such 2D materials is still open-ended, which demands detailed study for the practical usage [15]. The basic fundamental electrochemical properties of these materials have been studied over the past decade for bio-molecule sensing applications. However, the lack of an energy bandgap of the materials mentioned above has hindered their performance in the current market, which urges to find other semiconducting 2D materials [16].

Siloxene, a direct bandgap semiconductor with 2D structural configuration was firstly reported by Wohler in 1863 and can be prepared via deintercalation of calcium from calcium silicide ($CaSi_2$) [17,18]. It has been discovered and utilized in electrochemical water splitting, and supercapacitor electrode material thanks to the surface-terminated functional groups such as oxygen, hydrogen, and hydroxyl groups with Si chains [19,20]. Unlike graphene planar structure, siloxene is a low-buckled structure as a result of the double bond rule (mixed of sp^2 and sp^3 hybridization bonds) [21–23]. Various types of the siloxene have been reported in accordance with the stoichiometric ratio of Si:H:O. In general, the stoichiometric ratio of Si:H:O of siloxene is 2:2:1 [24]. Two types of siloxene structure have been confirmed in literatures; 1. Weiss-type structure ($Si_6(OH)_3H_3$), wherein alternating Si-OH and Si-H bonds are present around Si_6 rings [25]. 2. Kautsky-type structure ($Si_6O_3H_6$), in which Si_6 rings are linked via Si-O-Si bridges [26,27]. Siloxene sheets have been experimentally explored as an electrode material for supercapacitor with excellent electrochemical features by Krishnamoorthy et al. [18]. Similarly, calcium-bridged siloxene anode material has improved the cyclability of the lithium-

* Corresponding author at: School of Microelectronics, Southern University of Science and Technology, Shenzhen 518055, China.
** Corresponding author at: Department of Chemistry, Southern University of Science and Technology, Shenzhen 518055, China.
E-mail addresses: xu.zx@sustech.edu.cn (Z.-X. Xu), wangf@sustech.edu.cn (F. Wang).

https://doi.org/10.1016/j.apmt.2019.100477
2352-9407/

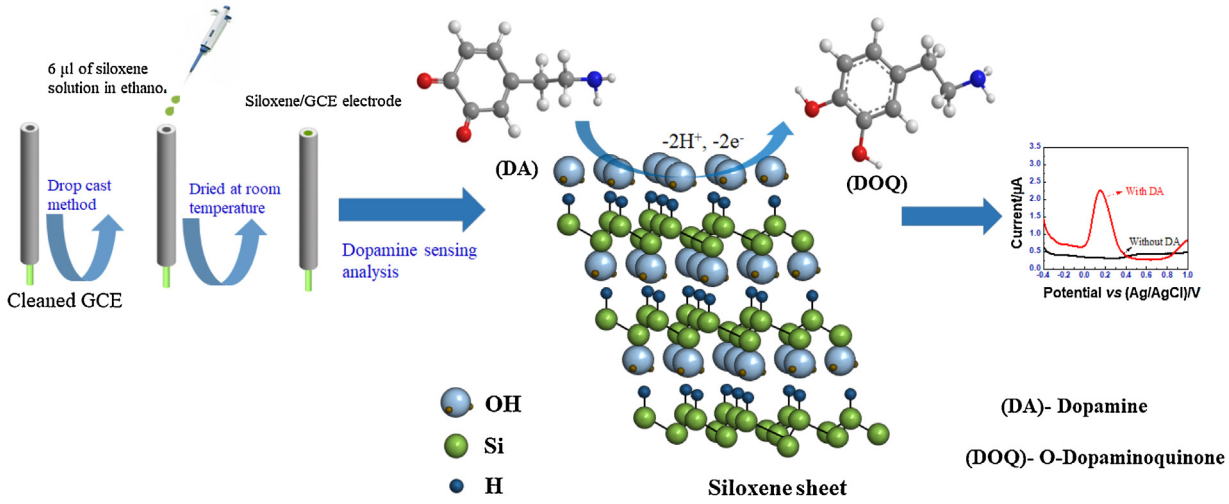

Scheme 1. Fabrication of siloxene/GCE modified electrode and plausible electrochemical oxidation mechanism of dopamine at siloxene surface.

ion battery [28]. Sun et al. reported carbon coated Silicon ($C@SiO_x$) from siloxene, which improved the Li-ion storage with high specific capacity of 760 mA h g^{-1} [29]. Thanks to the planar Si structure with the interconnection of Si_6 rings and various functional groups and its extremely large surface area, we anticipate that siloxene could possess several merits in the development of biosensors applications.

Dopamine (DA) is a catecholamine family neurotransmitter that has a crucial function in the human central nervous system and cardiovascular systems [30,31]. The imbalance or abnormal metabolisms of DA may lead to several diseases such as cancer, Parkinson, Huntington, and dementia [32]. Therefore, the facile detection and monitoring of DA are essential, which has received significant interest in the biosensing field. A variety of methods have been explored for the selective detection of dopamine, including chemiluminescence [33], gas chromatography-mass spectrometry [34], colorimetry [35], capillary electrophoresis [36] and electrochemical method [37]. Among them, the electrochemical detection technique is more adaptable for dopamine sensing thanks to its rapid response, high sensitivity, good selectivity, and low-cost [38]. On account of the better electrochemical active properties of the dopamine, the electrochemical technique has been known to be an effective method for high accuracy and low-cost detection of DA [39].

However, the electrochemical quantification of DA encounters a couple of major problems. One is electrode fouling upon oxidation, and the next one is the interference of several other biological molecules due to their overlapping potentials, leading to poor selectivity and reusability [40]. For example, the interfering compounds such as uric acid (UA) and ascorbic acid (AA) molecules possess the same oxidation potential that can be interfered during the detection of DA, which influences the selectivity and reproducibility of the electrode [41]. Till date, numerous strategies have been made to solve these drawbacks, which includes the various surface modifications on the electrode, finding new material for making electrodes and new electrochemical techniques [42]. Taking account of the issues above, the design, and synthesis of new electrode material is a primary task, which would be extremely beneficial for the development of cost-effective electrochemical sensor with high selectivity and wide linear range of detection.

From this perspective, in this work, we have explored the electrochemical activity of siloxene for the detection of DA. Siloxene is synthesized and used to modify glassy carbon electrode, where DA is electrochemically oxidized, as shown in Scheme 1. The dopamine is oxidized to form o-dopaminoquinone (DOQ) in aqueous solution at the surface of the siloxene with two-electron oxidation and two-protons of the hydroxyl groups [43]. Similar to the graphene, the oxygen-containing groups in siloxene play a vital role in the electrochemical oxidation of DA. The surface oxygen and hydroxyl groups at the basal and edge plane of the 2D siloxene can provide multiple electro-active sites for dopamine [44], which could greatly facilitate the electron transfer between the electrode and electro-active species. Therefore, detection of the sensing current reflects the DA content.

To the best of our knowledge, this is the first attempt to utilize siloxene in the electrochemical sensor applications, especially for dopamine determination. The siloxene sheets have been synthesized via deintercalation of calcium from calcium silicide and investigated its electrochemical dopamine sensing response by differential pulse voltammetry (DPV) technique. The proposed sensor exhibited a low detection limit with a wide linear range and good selectivity.

2. Experimental section

2.1. Preparation of siloxene sheets

The two-dimensional siloxene sheets were prepared via deintercalation of calcium from Calcium disilicide ($CaSi_2$, purchased from Alfa Asear, China) in Hydrochloric acid (HCl, 37% assay) solution. Briefly, 0.8 g of $CaSi_2$ powder was immersed in 100 mL of HCl solution at 0 °C with continuous stirring for four days under nitrogen atmosphere. Afterward, the yellowish green solid powder was centrifuged (Scheme 2) and washed with acetone for twelve times. Finally, the obtained product was dried at 80 °C under vacuum condition.

2.2. Materials characterization

Powder X-ray diffraction (XRD) pattern of siloxene and $CaSi_2$ samples were collected by Rigaku Smartlab diffractometer. Cu-Kα radiation (λ = 1.540 Å) was utilized to characterize the samples with the 2θ interval from 6 to 70°. The functional groups of siloxene were identified by Fourier transform infrared spectroscopy (FTIR, IR Tracer-100, Shimadzu, Japan). Scanning electron microscope (SEM, Zeiss Merlin) and Transmission electron microscope (TEM, Tecnai F 30) were used to identify the structural morphology of the siloxene. The thickness of siloxene sheets was determined by Atomic-force microscopy (AFM, 5500 AFM/STM) in tapping mode. Brunauer–Emmett–Teller (BET) textural characteristic of the sam-

Please cite this article as: R. Ramachandran, X. Leng, C. Zhao, et al., 2D siloxene sheets: A novel electrochemical sensor for selective dopamine detection, Appl. Mater. Today, https://doi.org/10.1016/j.apmt.2019.100477

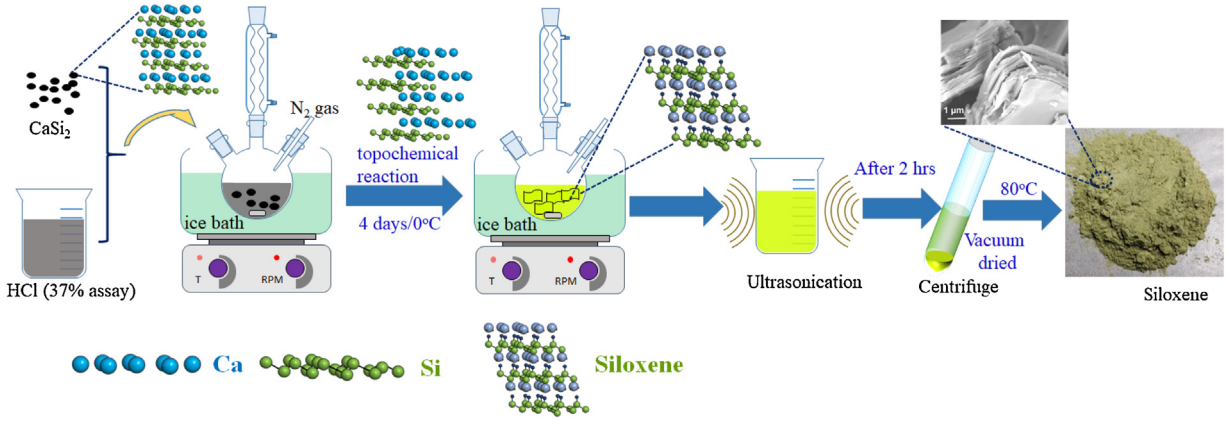

Scheme 2. Synthesis of the siloxene sheets through deintercalation of calcium from calcium disilicide.

ple was recorded by BET-ASAP2020. The surface elements and their chemical states of the sample were identified by X-ray photoelectron spectroscopy (XPS, ESCALB 250Xi) with Mg K radiation. Contact angle analyzer (Dataphysics, OCA-20, Germany) was used to measure the water wettability on the siloxene surface.

2.3. Preparation of siloxene modified glassy-carbon electrode (siloxene/GCE)

Typically, a bare glassy-carbon electrode was well-polished with alumina powder (0.05 μm). After polishing, the electrode was sonicated successively in distilled water and ethanol for 10 min. Then, the cleaned electrode was left to dry in the room temperature. Subsequently, 5 mg of the siloxene was taken in 50 μL Nafion (5% w/w in water and 1-propanol) containing 5 mL of ethanol and sonicated for 30 min. After that, 6 μL of the prepared siloxene solution was coated on the cleaned electrode by the drop-casting method using a micropipette and dried at room temperature (Scheme 1). 0.1 M of phosphate buffer solution (PB) with pH 7.0 was used as an electrolyte, and the dopamine sensing performance was analyzed using cyclic voltammetry (CV) and Differential pulse voltammetry (DPV) techniques.

3. Results and discussion

3.1. Formation of the siloxene sheets

The topotactic conversion of Zintl phase $CaSi_2$ into two-dimensional siloxene sheets by HCl is presented in Scheme 2. Deintercalation of calcium from $CaSi_2$ together with the functionalization of the siloxene sheets (oxygen and hydroxyl groups) co-occurred during the reaction which can be identified from a color change (black to yellow-greenish) confirming the formation of siloxene sheets [18]. The formation reaction of the siloxene can be expressed by the following equation [25],

$$3CaSi_2 + 6HCl + 3H_2O \rightarrow Si_6O_3H_6 + 3CaCl_2 + 3H_2 \uparrow \quad (1)$$

3.2. Characterization of the as-prepared siloxene

X-ray diffraction (XRD) was used to characterize the crystal structure of the as-prepared siloxene, and the obtained outcome is compared with $CaSi_2$. From Fig. 1, the sharp diffraction peaks of $CaSi_2$ are in good agreement with JCPDS card number 75-2192 [18,20]. The XRD pattern of siloxene shows broader peaks centered at 13.7 and 24° accompanied with sharp peaks at 28.5, 47.2, and 56.1°. The former ones are associated with the siloxene phase, which denotes the transformation of siloxene from calcium disilicide [45]. The sharp peaks (indicated as *) correspond to the common impurity (crystalline silicon) in $CaSi_2$. The same impurity peaks were reported previously by Dahu et al. [46].

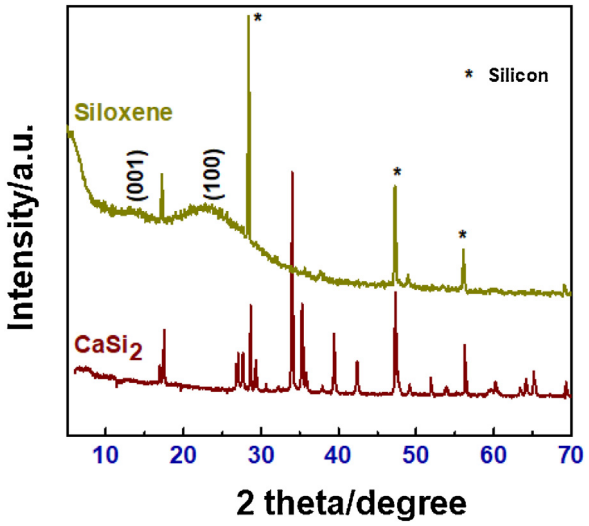

Fig. 1. XRD patterns of $CaSi_2$ and siloxene.

The specific surface area measurement and the porous nature of the as-synthesized siloxene were evaluated by N_2 adsorption-desorption isotherms analysis. As shown in Fig. 2(a), the prepared siloxene exhibits type IV isotherm with H3 type of hysteresis. The sharp climbing hysteresis loop at the high relative pressure (P/P_o) between 0.8 to 1.0 demonstrates the existence of the mesoporous behaviour [47], which attributes to the slit-like pores of siloxene. The formation of such slit-like pores is as a consequence of aggregated siloxene sheets. A similar phenomenon has been reported for graphene platelets [48,49]. The specific surface area of the siloxene is measured to be 30.89 $m^2 g^{-1}$. And the corresponding pore size distribution is calculated from the desorption branch by the Barrett-Joyner-Halenda (BJH) method, which further confirms the mesoporosity behaviour. From the inset of Fig. 2(a), it is estimated that the peak centered at around 4 nm, which is the optimal pore size for the ions penetration directly into the surface of the active electrode material. Thus, the siloxene sheets with open porous structure and high surface area can offer considerably more active sites for electrochemical reactions.

The functional group's attachment of siloxene during the topotactic reaction was confirmed through FTIR analysis. The transmittance spectrum is presented in Fig. 2(b). The characteristic peaks at 445, 876, 1052, and 1634 cm^{-1} correspond to the vibrations of

Please cite this article as: R. Ramachandran, X. Leng, C. Zhao, et al., 2D siloxene sheets: A novel electrochemical sensor for selective dopamine detection, Appl. Mater. Today, https://doi.org/10.1016/j.apmt.2019.100477

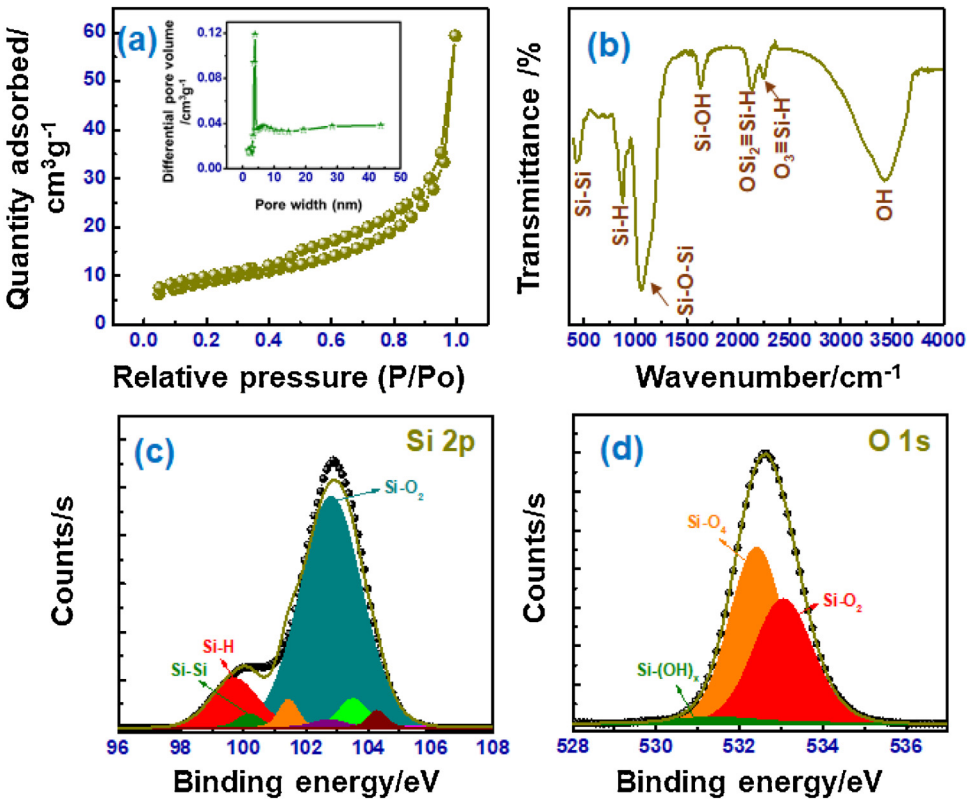

Fig. 2. (a) N_2 adsorption-desorption isotherms at 77 K and BJH pore size distribution curve (inset picture) of siloxene (b) FTIR spectrum of as-prepared siloxene (c and d) Core-level XPS spectrum of Si 2p and O 1s of siloxene.

υ (Si-Si), υ (Si-H), υ (Si—O—Si), and υ (Si-OH), respectively. A band at 2138 cm^{-1} associated with υ (OSi_2≡Si—H) mode can be found clearly, which indicates a Kautsky-type structure [18,26]. The presence of the bands at 2251 and 3409 cm^{-1} can be associated with the modes of $\upsilon(O_3$≡Si—H) and υ(—OH) [28]. This study confirms that most of the surface in siloxene has undergone oxidation and hydroxylation. Since the functional groups have been proved to be beneficial to the biomolecule's functionalization during biosensing [50,51], the presence of oxygen and hydroxyl groups in siloxene could improve the electrocatalytic oxidation process of dopamine sensing.

The elements, as well as their chemical composition states in the prepared siloxene sheets, were further studied by XPS analysis. The survey scan of the siloxene is given in Fig. S1, and the spectrum validates the presence of Si and O elements. It is noteworthy to mention that no peak has been recognized in the binding energy from 300 to 400 eV, which suggests the complete removal of Ca element from $CaSi_2$ during the topotactic reaction. Furthermore, the core-level spectrum of Si 2p (Fig. 2c) has significant peaks at 99.6, 100.1 and 102.8 eV, which can be assigned to the characteristic peaks of Si-H, Si-Si and Si-O_2 of 2D silicon network, respectively [52,19]. The existence of the elemental (Si-Si) at the lower binding energy is due to the impurity in the $CaSi_2$ precursor. However, the intensity of the Si-Si mode is weak and can be negligible. Besides, the fitted Si-O_2 region consists of the additional characteristic peaks which reveal the occurrence of different oxidation states of Si probably from silicon suboxides network [53]. The oxygenated and hydroxyl-functionalized counterparts of as-prepared siloxene were confirmed by the O 1s spectrum (Fig. 2d). In the deconvolved spectrum, the binding energy located at 531.1, 532.4, and 533.0 eV corresponding to Si-$(OH)_x$, Si-O_4 and Si-O_2 bonds of two-dimensional Si chain networks, respectively [54]. The ratio of O/Si atoms in the siloxene is found to be 1.54 from the XPS analysis, which agrees well with previously reported work [55].

The structural morphology of the siloxene was studied with the scanning electron microscope and transmission electron microscope. The SEM images of the siloxene revealed that the multi-layer stacked structure with interlayered voids (mentioned in Fig. 3a). The existence of the voids between the layers could be beneficial for fast electrolyte ion diffusion during the electrochemical redox reactions. Fig. 3(c and d) shows the TEM images of siloxene, which demonstrates its sheet-like structure with the dimension from a few nm to micrometers. Furthermore, the occurrence of the elements in siloxene was analyzed by SEM mapping and energy dispersive X-ray spectroscopy (EDS) analysis. In Fig. 4, a homogenous distribution of Si and O atoms can be observed throughout the prepared siloxene. The EDS spectrum confirms the presence of Si and O elements in siloxene.

Atomic microscopic image of siloxene sheets coated on cleaned Si wafer is presented in Fig. 5. The large-scale image (Fig. 5a) reveals the two-dimensional thin sheet-like structure of siloxene. As can be seen in section analysis, the majority of sheet exhibits uniform morphology with a thickness of around 6 nm, which demonstrates the few-layers of siloxene. The 3D view of the image (Fig. 5b) further validates the uniformity of the siloxene. It should be noted that, a few of the thick sheets (thickness more than 15 nm) have also been observed in the sample probably due to the unexfoliated region of siloxene.

The water wettability on the siloxene surface was measured by the contact angle method, as shown in Fig. S2. Compared to the bare glass substrate with a relatively hydrophilic surface (contact angle $36.2 \pm 1.1^\circ$), the siloxene coated glass surface exhibited the contact angle of $127.7 \pm 1.2^\circ$, which implies the hydrophobic nature of the siloxene.

Please cite this article as: R. Ramachandran, X. Leng, C. Zhao, et al., 2D siloxene sheets: A novel electrochemical sensor for selective dopamine detection, Appl. Mater. Today, https://doi.org/10.1016/j.apmt.2019.100477

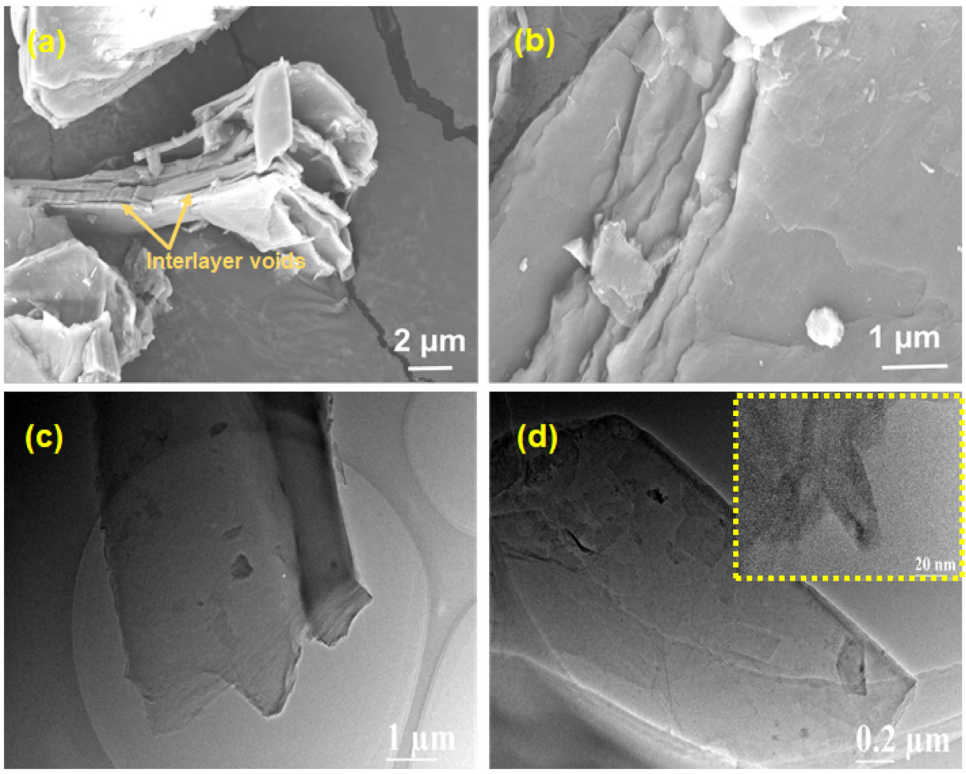

Fig. 3. (a, b) Scanning electron microscopic images and (c, d) Transmission electron microscopy images of the siloxene. The inset picture shows the high-resolution TEM image of siloxene.

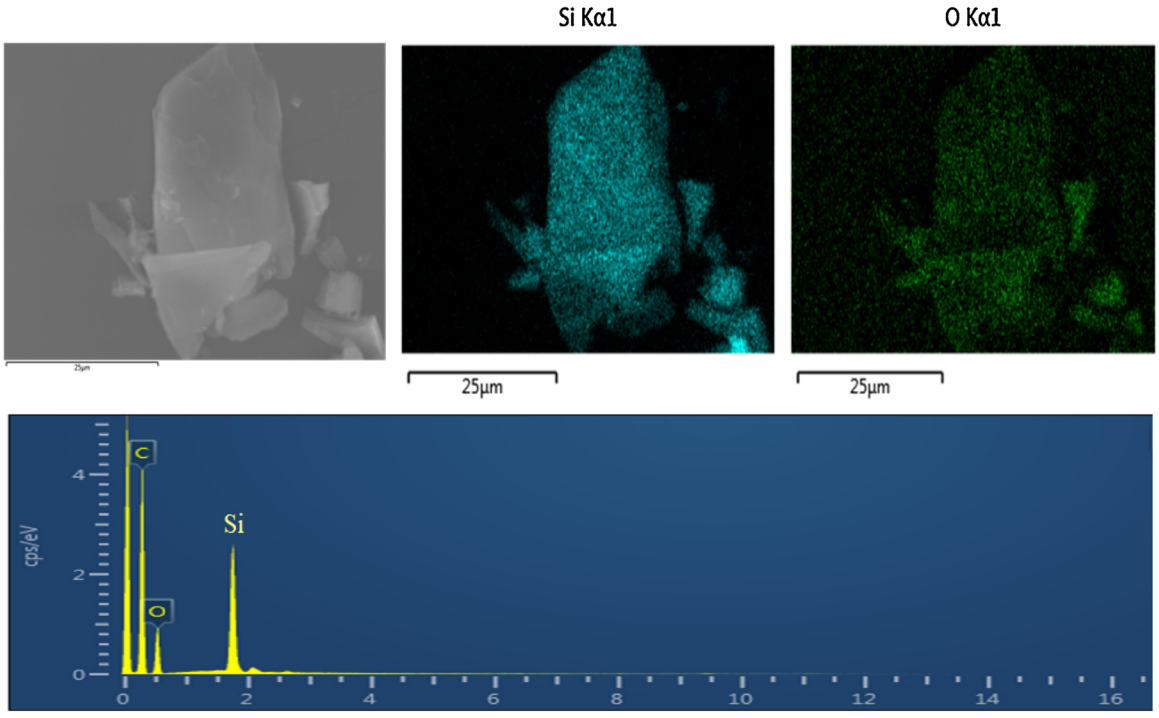

Fig. 4. Elemental mapping and the EDS spectrum of as-prepared siloxene sheets.

3.3. Electrochemical studies of dopamine sensing

3.3.1. Electrochemical behaviour of siloxene/GCE electrode

Electrochemical impedance spectroscopy (EIS) is useful to review the surface conductivity changes of the bare glassy-carbon electrode (GCE) and the modified electrode. Fig. 6(a) shows the Nyquist plot of bare GCE and siloxene modified GCE in 0.1 M of $[Fe(CN)_6]^{3-/4-}$ contain 0.1 M of KCl electrolyte medium. The Nyquist plot of EIS includes a semicircle at the high-frequency region which refers to the electron transfer limiting process, and the value of the semicircle diameter is known as charge transfer resistance (R_{ct}) [56]. A linear straight line at the low-frequency

Please cite this article as: R. Ramachandran, X. Leng, C. Zhao, et al., 2D siloxene sheets: A novel electrochemical sensor for selective dopamine detection, Appl. Mater. Today, https://doi.org/10.1016/j.apmt.2019.100477

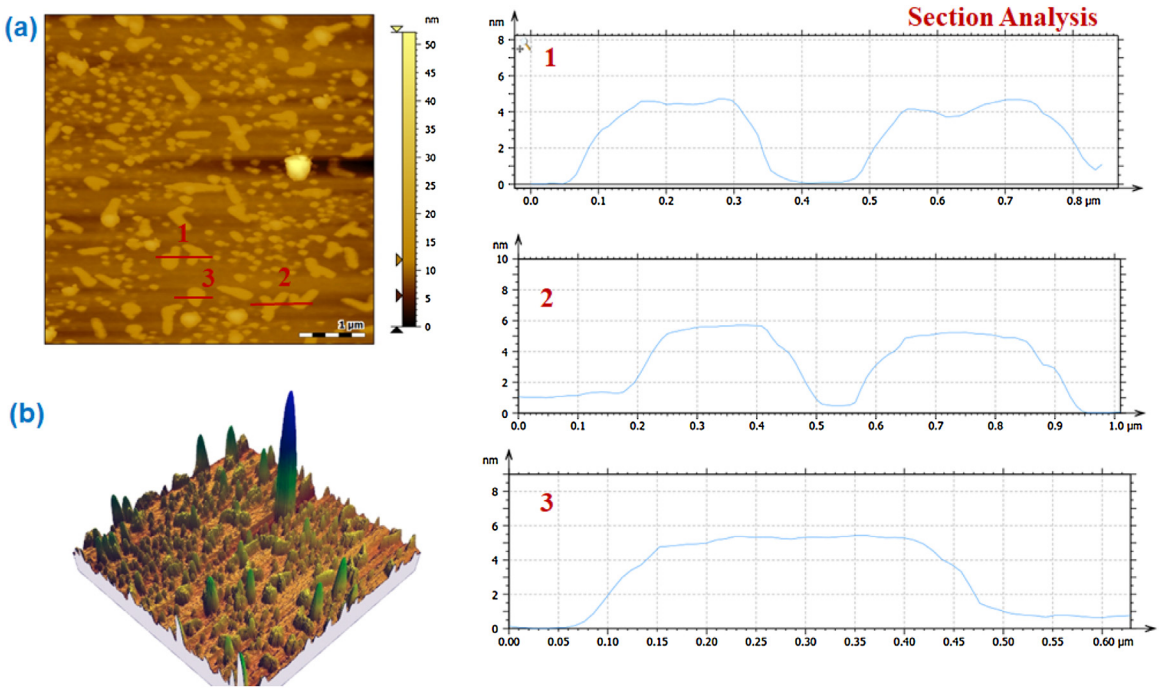

Fig. 5. AFM images of siloxene sheets coated Si wafer (a) topography image (b) 3D view.

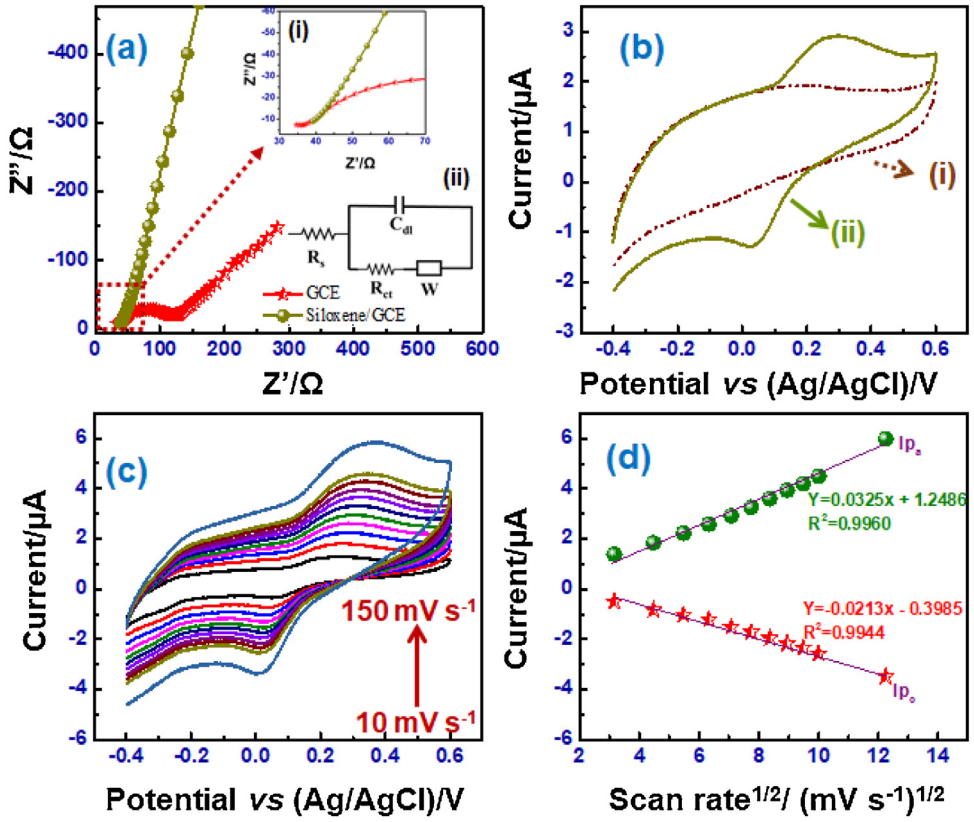

Fig. 6. (a) Nyquist plots of bare GCE and siloxene modified GCE in 0.1 M of $[Fe(CN)_6]^{3-/4-}$ containing 0.1 M of KCl electrolyte. (Inset images: (i) Enlarged Nyquist plot and (ii) Randles circuit model) (b) CV response of the modified electrode in 0.1 M PB solution (i) Absence of 400 μM DA and (ii) Presence of 400 μM DA (c) CV response of the siloxene modified electrode at different scan rates in the presence of 400 μM DA containing 0.1 M PB solution (d) Calibration curve of the anodic and cathodic peak current versus square root of the scan rate.

region is associated with the diffusion-controlled process [57]. From Fig. 6(a), the bare GCE displayed a large semicircle that indicates the higher resistivity behaviour. Whereas after coated with siloxene, the semicircle can be barely seen at the high frequency region shown in the enlarged inset picture (i) of Fig. 6(a), which reveals the low faradic charge transfer resistance. Besides,

Please cite this article as: R. Ramachandran, X. Leng, C. Zhao, et al., 2D siloxene sheets: A novel electrochemical sensor for selective dopamine detection, Appl. Mater. Today, https://doi.org/10.1016/j.apmt.2019.100477

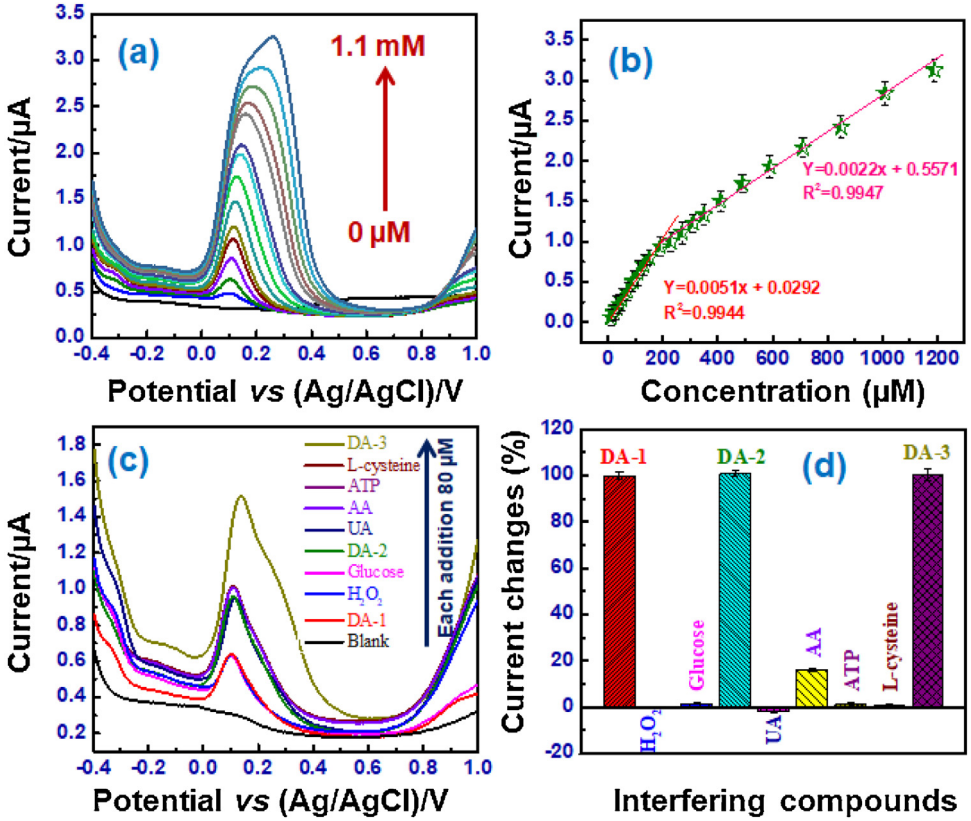

Fig. 7. (a) DPV response of the siloxene/GCE electrode in 0.1 M PB solution containing different concentration of DA (b) Linear response of the oxidation current versus DA concentrations (c) Interference analysis of siloxene/GCE electrode in the presence of other interfering compounds (d) Current changes response of the interfering compounds (H_2O_2 – hydrogen peroxide, glucose, UA – Uric acid, AA – Ascorbic acid, ATP – Adenosine triphosphate and L-cysteine).

the linear portion is almost parallel to the y-axis, which might attribute to the high electron conduction process between the electrode/electrolyte interface. The Randles circuit was used for fitting the impedance data, as shown in the inset (ii) of Fig. 6(a). From the circuit, R_s, R_{ct}, C_{dl}, and W represents the solution resistance, charge transfer resistance, double-layer capacitance and Warburg impedance, respectively. The R_{ct} value of bare GCE and siloxene/GCE electrodes are estimated to be 67.6 Ω and 9.1 Ω, respectively. These observations demonstrate that the modification of GCE with siloxene could increase the conductivity during the electrochemical redox reactions.

The electrochemical catalytic behaviour of siloxene modified GCE electrode before and after addition of 400 μM DA in 0.1 M PB solution was recorded by CV technique as shown in Fig. 6(b). The siloxene/GCE electrode shows a well-defined redox peak response (indicated as (ii) in Fig. 6b) after the addition of DA. This result confirms the superior electrocatalytic activity of the siloxene sheet towards DA detection.

The electrochemical kinetics of DA sensing on the modified electrode at various scan rates in 400 μM of DA-containing 0.1 M PB solution were further evaluated by CV measurements. As from Fig. 6(c), the anodic and cathodic peak currents (Ip_a and Ip_c) increase significantly with increasing scan rates. On the other hand, the redox peak potential is shifted towards positive and negative at higher scan rates, which demonstrates the fast electron transfer phenomenon between the modified electrode and DA [58]. Besides, the calibration graph is drawn among the redox peak currents and the square root of the scan rates shown in Fig. 6(d). A linear increase in both anodic and cathodic peak currents with the square root of the scan rate reveals the diffusion-controlled electrochemical redox reaction of DA at siloxene modified GCE electrode [59].

3.3.2. Detection of DA at siloxene modified GC electrode

Since the DPV method affords several advantages in comparison with other electrochemical processes such as high sensitivity, rapid response, and the wide linear range [60], the DPV technique was applied to recognize the selective DA detection of the proposed modified electrode under the optimal experimental conditions. Fig. 7(a) exhibits the DPV response of the siloxene modified electrode in the presence of various DA concentrations in the PB solution. From the DPV profile, the oxidation peak current response of the siloxene modified electrode increases gradually with the addition of DA from 0 μM to 1.1 mM, which proves the excellent electrocatalytic activity of the layered siloxene structure towards the DA oxidation process. Besides, a linear relationship is attained between the oxidation peak current and the concentration of DA with two linear ranges (Fig. 7(b)) i.e., the first linear range is observed from 10 to 190 μM (lower concentration range) with the correlation coefficient of $R^2 = 0.9944$ and the second linear range from 200 μM to 1.1 mM with R^2 value 0.9947 (higher concentration range). The sensitivity and limit of detection (LOD) of the siloxene/GCE electrode for DA detection were determined at lower linear response region, and the estimated sensitivity and LOD of DA oxidation is about 0.0728 μA μM^{-1} cm^2 and 0.327 μM, respectively. Our siloxene/GCE modified electrode shows superior detection of DA with a lower detection limit, the comparison of the analytical performance of previously reported DA sensors is made and given in the Table 1.

3.3.3. Effect of potentially interfering substances

Selectivity is an essential characteristic of the electrochemical sensors for practical application. The selectivity of the fabricated sensor in the presence of interfering compounds has been inves-

Please cite this article as: R. Ramachandran, X. Leng, C. Zhao, et al., 2D siloxene sheets: A novel electrochemical sensor for selective dopamine detection, Appl. Mater. Today, https://doi.org/10.1016/j.apmt.2019.100477

Table 1
Analytical performance characteristics for other two-dimensional electrochemical sensors reported for dopamine detection.

Electrode[a]	Technique	LOD (μM)	Linear range (μM)	Ref
ERGO/GCE	DPV	0.50	0.5–60	[61]
AG/GCE	DPV	0.33	0.5–35	[62]
G/SnO_2/GCE	DPV	1.0	2–100	[63]
rGO/CeO_2/GCE	DPV	10	10–150	[64]
rGO/TiO_2	DPV	1.5	1–35; 35–100	[65]
N-RGO/MnO	DPV	3.0	10–180	[66]
N-RGO/GCE	LSV	0.93	120–220	[67]
Ag/Graphene/GCE	LSV	5.4	10–800	[68]
Bi/GNS/GCE	Amperometry	0.35	1–30	[69]
SiO_2/C/CuPc	Amperometry	0.60	10–140	[70]
Siloxene/GCE	**DPV**	**0.327**	**10–190; 200–1100**	**This work**

[a]ERGO – Electrochemically reduced graphene oxide; AG – Activated graphene; G – Graphene; rGO – Reduced graphene oxide; N-RGO – Nitrogen-doped graphene oxide; GNS – Graphene nanosheet; CuPc – Copper phthalocyanine.

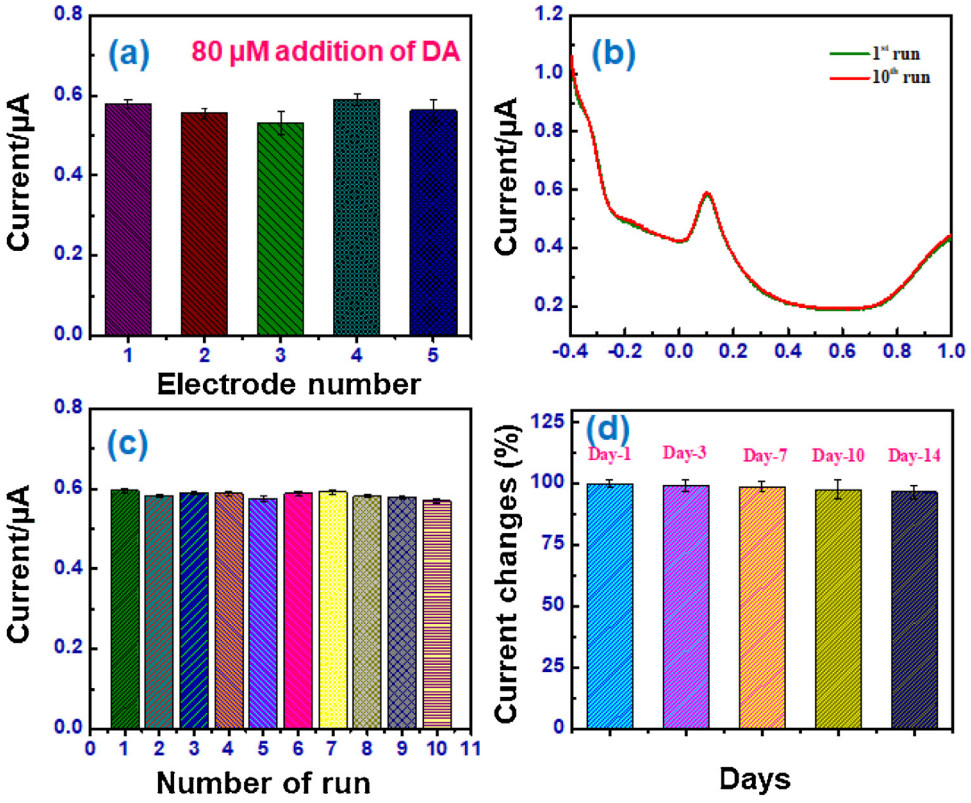

Fig. 8. (a) The reproducibility of siloxene modified electrode for five different electrodes (b) Repeatability of a modified electrode in the presence of 80 μM of DA-containing 0.1 M PB solution (c) plot of the oxidation current versus the number of a run for ten consecutive measurements (d) Stability of the modified electrode.

tigated by DPV method. Fig. 7(c) reveals the DPV response of the siloxene modified electrode in the presence of DA with other interfering species like glucose, H_2O_2, UA, AA, ATP, and L-cysteine. As can be seen from Fig. 7(c), the initial current response is observed according to the addition of 80 μM of DA. Afterward, 80 μM of H_2O_2 followed by 80 μM glucose are injected successively, while no significant difference could be found in the oxidation current of the proposed sensor. Then, the second addition of 80 μM DA is added into the PB solution containing glucose and H_2O_2 interfering species, and remarkable change can be seen in the oxidation current, which indicates the good selectivity of the sensor. Furthermore, the other interfering compounds (UA, AA, ATP and L-cysteine) have also been injected (80 μM concentration of each compound), showing negligible current response compared with DA oxidation current level (Fig. 7d). This demonstrates the good selectivity of the proposed siloxene/GCE sensor for DA detection and it could be used for the selective real-time DA detection. The detection mechanism of siloxene has not been investigated yet. Based on our experimental results, we assume that the enhanced and selective response of DA sensing by the siloxene probably associated to the following reason. Since siloxene possesses a two-dimensional low-buckled structure, the π-π interaction between the DA phenyl structure and siloxene planar structure results in potential electron transfer during DA oxidation. Whereas, the π-π interaction of siloxene with other interfering molecules like AA and UA is weak, lead to inactive oxidation. A similar phenomenon has been described for graphene-based modified electrodes to DA sensing [71,72].

3.3.4. *Reproducibility, repeatability, and stability*

To evaluate the reproducibility of the siloxene/GCE sensor, five modified electrodes were fabricated in similar condition and utilized for detection of 80 μM of DA-containing PB solution by DPV. From Fig. 8(a), all the five electrodes exhibit similar oxidation current response with a relative standard deviation (RSD) of 2.8%, which is the acceptable reproducibility of the sensors. The proposed sensor not only displays an excellent reproducibility but

Please cite this article as: R. Ramachandran, X. Leng, C. Zhao, et al., 2D siloxene sheets: A novel electrochemical sensor for selective dopamine detection, Appl. Mater. Today, https://doi.org/10.1016/j.apmt.2019.100477

also exposes promising repeatability for DA detection. As shown in Fig. 8(b and c), the oxidation current response of DA is almost identical for ten replicate measurements, which indicates the excellent repeatability feature of the sensor. Since the long-term analysis of the sensor is another crucial factor, the DPV was investigated to determine the stability of the proposed sensor. The electrode was stored in the refrigerator when not in use. Fig. S3 shows the DPV response of the modified electrode in the presence of 200 μM of DA. It is noted that the DA oxidation current of the electrode decreases slightly after 14 days when compared with the initial measurement. As shown in Fig. 8(d), the current response of the modified electrode remains up to 96.3% even after two weeks, which shows the excellent stability of the sensor for DA detection. Based on our primary results, 2D siloxene modified electrode is a promising candidate for the selective detection of dopamine.

4. Conclusion

In summary, two-dimensional siloxene sheets have been successfully prepared from calcium disilicide through topotactic reaction and confirmed from the various characterization techniques. A novel siloxene modified glassy-carbon electrode was fabricated and applied for selective determination of dopamine. The proposed sensor exhibited remarkable electrocatalytic activity towards dopamine sensing with a detection limit of 0.327 μM and a wide linear range (10–190 μM; 200–1100 μM). Besides, the sensor presented excellent reproducibility, along with good repeatability and stability. It is believed that siloxene based electrode will be a potential choice for constructing sensitive and selective dopamine sensing platform. The further optimization process of the siloxene will be investigated to heighten the electrochemical sensing activity in the future.

Acknowledgements

This work was supported by Special Funds for the Development of Strategic Emerging Industries in Shenzhen (JCYJ20170818154457845, 2017) and Shenzhen Science and Technology Innovation Committee (Projects No. JCYJ20170412154426330). Fei Wang is supported by Guangdong Natural Science Funds for Distinguished Young Scholar (Projects No. 2016A030306042), and the Guangdong Special Support Program under (Projects No. 2015TQ01X555).

Appendix A. Supplementary data

Supplementary material related to this article can be found, in the online version, at doi:https://doi.org/10.1016/j.apmt.2019.100477.

References

[1] X. Kong, Q. Liu, C. Zhang, Z. Peng, Q. Chen, Elemental two-dimensional nanosheets beyond graphene, Chem. Soc. Rev. 46 (2017) 2127–2157.
[2] J. Sturala, Z. Sofer, M. Pumera, Chemistry of layered pnictogens: phosphorus, arsenic, antimony, and bismuth, Angew. Chem. Int. Ed. 58 (2019) 7551–7557.
[3] R.S. Edwards, K.S. Coleman, Graphene synthesis: relationship to applications, Nanoscale 5 (2013) 38–51.
[4] R. Ramachandran, S. Felix, G.M. Joshi, B.P.C. Raghupathy, S.K. Jeong, A.N. Grace, Synthesis of graphene platelets by chemical and electrochemical route, Mater. Res. Bull. 48 (2013) 3834–3842.
[5] J. Kang, Q. Su, H. Feng, P. Huang, G. Du, B. Xu, $MoSe_2$ nanosheets-wrapped flexible carbon cloth as binder-free anodes for high-rate lithium and sodium ion storages, Electrochim. Acta 301 (2019) 29–38.
[6] A.K. Singh, P. Kumar, D.J. Late, A. Kumar, S. Patel, J. Singh, 2D layered transition metal dichalcogenides (MoS_2): synthesis, applications and theoretical aspects, Appl. Mater. Today 13 (2018) 242–270.
[7] Z.G. Yu, Y.W. Zhang, B.I. Yakobson, Phosphorene-based nanogenerator powered by cyclic molecular Doping, Nano Energy 23 (2016) 34–39.
[8] L. Wang, M. Pumera, Electrochemical catalysis at low dimensional carbons: graphene, carbon nanotubes and beyond – a review, Appl. Mater. Today 5 (2016) 134–141.
[9] M. Aliramezani, C.R. Koch, M. Secanell, R.E. Hayes, R. Patrick, An electrochemical model of an amperometric NOx sensor, Sens. Actuators B 290 (2019) 302–311.
[10] R. Kumuthini, R. Ramachandran, H.A. Therese, F. Wang, Electrochemical properties of electrospun MoS_2@C nanofiber as electrode material for high-performance supercapacitor application, J. Alloys Compd. 705 (2017) 624–630.
[11] S. Xu, Z. Lei, P. Wu, Facile preparation of 3D MoS_2/$MoSe_2$ nanosheet–graphene networks as efficient electrocatalysts for the hydrogen evolution reaction, J. Mater. Chem. A 3 (2015) 16337–16347.
[12] S. Ramalingam, R. Chand, C.B. Singh, A. Singh, Phosphorene-gold nanocomposite based microfluidic aptasensor for the detection of okadaic acid, Biosens. Bioelectron. 135 (2019) 14–21.
[13] A. Naseri, M. Samadi, A. Pourjavadi, A.Z. Moshfegh, S. Ramakrishna, Graphitic carbon nitride (g-C_3N_4)-based photocatalysts for solar hydrogen generation: recent advances and future development directions, J. Mater. Chem. A 5 (2017) 23406–23433.
[14] P.A. Rasheed, R.P. Pandey, K. Rasool, K.A. Mahmoud, Ultra-sensitive electrocatalytic detection of bromate in drinking water based on Nafion/$Ti_3C_2T_x$ (MXene) modified glassy carbon electrode, Sens. Actuators B 265 (2018) 652–659.
[15] H. Li, Y. Hou, F. Wang, M.R. Lohe, X. Zhuang, L. Niu, X. Feng, Flexible all-solid-state supercapacitors with high volumetric capacitances boosted by solution processable MXene and electrochemically exfoliated graphene, Adv. Energy Mater. 7 (2017), 1601847.
[16] M. Velicky, P.S. Toth, From two-dimensional materials to their heterostructures: an electrochemist's perspective, Appl. Mater. Today 8 (2017) 68–103.
[17] F. Wöhler, Ueber Verbindungen des Siliciums mit Sauerstoff und Wasserstoff, Justus Liebigs Ann. Chem. 127 (1863) 257–274.
[18] K. Krishnamoorthy, P. Pazhamalai, S.J. Kim, Two-dimensional siloxene nanosheets: novel high-performance supercapacitor electrode materials, Energy Environ. Sci. 11 (2018) 1595–1602.
[19] S. Li, H. Wang, D. Li, X. Zhang, Y. Wang, J. Xie, J. Wang, Y. Tian, W. Ni, Y. Xie, Siloxene nanosheets: a metal-free semiconductor for water splitting, J. Mater. Chem. A 4 (2016) 15841–15844.
[20] P. Pazhamalai, K. Krishnamoorthy, S. Sahoo, V.K. Mariappan, S.J. Kim, Understanding the thermal treatment effect of two-dimensional siloxene sheets and the origin of superior electrochemical energy storage performances, ACS Appl. Mater. Interfaces 11 (2019) 624–633.
[21] J. Zhao, H. Li, Z. Yu, R. Quhe, S. Zhou, Y. Wang, C.C. Liu, H. Zhong, N. Han, J. Lu, Y. Yao, K. Wu, Rise of silicene: a competitive 2D material, Prog. Mater. Sci. 83 (2016) 24–151.
[22] T. Hartman, Z. Sofer, Beyond graphene: chemistry of group 14 graphene analogues: silicene, germanene, and stanene, ACS Nano 13 (2019) 8566–8576.
[23] A. Molle, C. Grazianetti, L. Tao, D. Taneja, Md.H. Alam, D. Akinwande, Silicene, silicene derivatives, and their device applications, Chem. Soc. Rev. 47 (2018) 6370–6387.
[24] Y. Wang, Y. Ding, Structural stability and the electronic properties of a $(SiH)_2O$-formed siloxene sheet: a computational study, Phys. Chem. Chem. Phys. 19 (2017) 18030–18035.
[25] A. Weiss, G. Beil, H. Meyer, The topochemical reaction of $CaSi_2$ to a two-dimensional subsiliceous acid $Si_6H_3(OH)_3$ (= Kautskys' siloxene), Z. Naturforsch. B; Anorg. Chem. Org. Chem. 34 (1979) 25–30.
[26] S. Yamanaka, H. Mastsu-ura, M. Ishikawa, New deintercalation reaction of calcium from calcium disilicide. Synthesis of layered polysilane, Mater. Res. Bull. 31 (1996) 307–316.
[27] H. Kautsky, W. Vogell, F. Oeters, Die Bedeutung elektronenmikroskopischer Untersuchungen für die Konstitutions-und Strukturaufklärung des Siloxens, Z. Naturforsch. B; Anorg. Chem. Org. Chem. Biochem. Biophys. Biol. 10 (1955) 597–598.
[28] H. Imagawa, N. Takahashi, T. Nonaka, Y. Kato, K. Nishikawa, H. Itahara, Synthesis of a calcium-bridged siloxane by a solid state reaction for optical and electrochemical properties, J. Mater. Chem. A 3 (2015) 9411–9414.
[29] L. Sun, T. Su, L. Xu, M. Liu, H.B. Du, Two-dimensional ultra-thin SiOx(0<x<2) nanosheets with long-term cycling stability as lithium ion battery anodes, Chem. Commun. 52 (2016) 4341–4434.
[30] H.-B. Wang, H.-D. Zhang, Y. Chen, K.-J. Huang, Y.-M. Liu, A label-free and ultrasensitive fluorescent sensor for dopamine detection based on double-stranded DNA templated copper nanoparticles, Sens. Actuators B 220 (2015) 146–153.
[31] J.A. Behan, F. Grajkowski, D.R. Jayasundara, L.V. Arribas, M.G. Melchor, P.E. Colavita, Influence of carbon nanostructure and oxygen moieties on dopamine adsorption and charge transfer kinetics at glassy carbon surfaces, Electrochim. Acta 304 (2019) 221–230.
[32] A.A. Grace, K.P. Divya, V. Dharuman, J.H. Hahn, Single step sol-gel synthesized Mn_2O_3-TiO_2 decorated graphene for the rapid and selective ultra-sensitive electrochemical sensing of dopamine, Electrochim. Acta 302 (2019) 291–300.
[33] H. Duan, L. Li, X. Wang, Y. Wang, J. Li, C. Luo, A sensitive and selective chemiluminescence sensor for the determination of dopamine based on silanized magnetic graphene oxide-molecularly imprinted polymer, Spectrochim. Acta A 139 (2015) 374–379.

Please cite this article as: R. Ramachandran, X. Leng, C. Zhao, et al., 2D siloxene sheets: A novel electrochemical sensor for selective dopamine detection, Appl. Mater. Today, https://doi.org/10.1016/j.apmt.2019.100477

[34] A. Naccarato, E. Gionfriddo, G. Sindona, A. Tagarelli, Development of a simple and rapid solid phase microextraction-gas chromatography–triple quadrupole mass spectrometry method for the analysis of dopamine, Anal. Chim. Acta 810 (2014) 17–24.
[35] L. Song, Y. Zhu, Z. Yang, C. Wang, X. Lu, Oxidase-mimicking activity of perovskite LaMnO3+δ nanofibers and their application for colorimetric sensing, J. Mater. Chem. B 6 (2018) 5931–5939.
[36] H. Fang, M.L. Pajski, A.E. Ross, B.J. Venton, Quantitation of dopamine, serotonin and adenosine content in a tissue punch from a brain slice using capillary electrophoresis with fast-scan cyclic voltammetry detection, Anal. Methods 5 (2013) 2704–2711.
[37] N. Diab, D.M. Morales, C. Andronescu, M. Masoud, W. Schuhmann, A sensitive and selective graphene/cobalt tetrasulfonated phthalocyanine sensor for detection of dopamine, Sens. Actuators B 285 (2019) 17–23.
[38] J. Jiao, J. Zuo, H. Pang, L. Tan, T. Chen, H. Ma, A dopamine electrochemical sensor based on Pd-Pt alloy nanoparticles decorated polyoxometalate and multiwalled carbon nanotubes, J. Electroanal. Chem. 827 (2018) 103–111.
[39] E.Y.L. Teo, G.A.M. Ali, H. Algarni, W. Cheewsaedtham, T. Rujiralai, K.F. Chong, One-step production of pyrene-1-boronic acid functionalized graphene for dopamine detection, Mater. Chem. Phys. 231 (2019) 286–291.
[40] B.B. Li, Y.S. Zhou, W. Wu, M. Liu, S.R. Mei, Y.K. Zhou, T. Jing, Highly selective and sensitive determination of dopamine by the novel molecularly imprinted poly(nicotinamide)/CuO nanoparticles modified electrode, Biosens. Bioelectron. 67 (2015) 121.
[41] M. Sarno, S. Galvagno, C. Scudieri, P. Iovane, S. Portofino, C. Borriello, C. Cirillo, Dopamine sensor in real sample based on thermal plasma silicon carbide nanopowders, J. Phys. Chem. Solids 131 (2019) 213–222.
[42] S.R. Ali, Y.F. Ma, R.R. Parajuli, Y. Balogun, W.Y.C. Lai, H.X. He, A nonoxidative sensor based on a self-doped polyaniline/carbon nanotube composite for sensitive and selective detection of the neurotransmitter dopamine, Anal. Chem. 79 (2007) 2583–2587.
[43] M. Zhang, C. Liao, Y. Yao, Z. Liu, F. Gong, F. Yan, High-performance dopamine sensors based on whole graphene solution-gated transistors, Adv. Funct. Mater. 24 (2014) 978–985.
[44] Y. Shao, J. Wang, H. Wu, J. Liu, I.A. Aksay, Y. Lin, Graphene based electrochemical sensors and biosensors: a review, Electroanalysis 22 (2010) 1027–1036.
[45] H. Nakano, O. Ohtani, T. mistsuoka, Y. Akimoto, H. Nakamura, Synthesis of amorphous silica nanosheets and their photoluminescence, J. Am. Ceram. Soc. 88 (2005) 3522–3524.
[46] J.R. Dahn, B.M. Way, E. Fuller, J.S. Tse, Structure of siloxene and layered polysilane (Si_6H_6), Phys. Rev. B 48 (1993) 17872–17877.
[47] R. Ramachandran, Q. Hu, F. Wang, Z.X. Xu, Synthesis of N-$CuMe_2Pc$ nanorods/graphene oxide nanocomposite for symmetric supercapacitor electrode with excellent cyclic stability, Electrochim. Acta 298 (2019) 770–777.
[48] S. Tang, S. Jiu, R. Zhang, Y. Liu, J. Wang, Z. Hu, W. Lu, S. Yang, W. Qiao, L. Ling, M. Jin, Effective reduction of graphene oxide via a hybrid microwave heating method by using mildly reduced graphene oxide as a susceptor, Appl. Surf. Sci. 473 (2019) 222–229.
[49] X. Zhao, Y. Jia, Z.H. Liu, GO-graphene ink-derived hierarchical 3D-graphene architecture supported Fe_3O_4 nanodots as high-performance electrodes for lithium/sodium storage and supercapacitors, J. Colloid Interface Sci. 536 (2019) 463–473.
[50] M. Pumera, Graphene in biosensing, Mater. Today 14 (2011) 308–315.
[51] D. Sharma, S. Kanchi, M.I. Sabela, K. Bisetty, Insight into the biosensing of graphene oxide: present and future prospects, Arabian J. Chem. 9 (2016) 238–261.
[52] G.M. Ingo, N. Zacchetti, D. Della Sala, C. Coluzza, X-ray photoelectron spectroscopy investigation on the chemical structure of amorphous silicon nitride (a-SiNx), J. Vac. Sci. Technol. A 7 (1989) 3048–3055.
[53] R. Fu, Y. Li, Y. Wu, C. Shen, C. Fan, Z. Liu, Controlling siloxene oxidization to tailor SiO_x anodes for high performance lithium ion batteries, J. Power Sources 432 (2019) 65–72.
[54] W. Zhang, L. Sun, J.M.V. Nsanzimana, X. Wang, Lithiation/delithiation synthesis of few layer silicene nanosheets for rechargeable Li–O_2 batteries, Adv. Mater. 30 (2018), 1705523.
[55] R. Fu, K. Zhang, R.P. Zaccaria, H. Huang, Y. Xia, Z. Liu, Two-dimensional silicon suboxides nanostructures with Si nanodomains confined in amorphous SiO_2 derived from siloxene as high performance anode for li-ion batteries, Nano Energy 39 (2017) 546–553.
[56] Z. Liu, M. Jin, J. Cao, R. Niu, P. Li, G. Zhou, Y. Yu, A.V.D. Berg, L. Shui, Electrochemical sensor integrated microfluidic device for sensitive and simultaneous quantification of dopamine and 5-hydroxytryptamine, Sens. Actuators B 273 (2018) 873–883.
[57] P. Balasubramanian, T.S.T. Balamurugan, S.M. Chen, T.W. Chen, P.H. Lin, A novel, efficient electrochemical sensor for the detection of isoniazid based on the B/N doped mesoporous carbon modified electrode, Sens. Actuators B 283 (2019) 613–620.
[58] J.V. Kumar, R. Karthik, S.M. Chen, N. Raja, V. Selvam, V. Muthuraj, Evaluation of a new electrochemical sensor for selective detection of non-enzymatic hydrogen peroxide based on hierarchical nanostructures of zirconium molybdate, J. Colloid Interface Sci. 500 (2017) 44–53.
[59] S. Kumar, Y. Lei, N.H. Alshareef, M.A. Quevedo-Lopez, K.N. Salama, Biofunctionalized two-dimensional Ti_3C_2 MXenes for ultrasensitive detection of cancer biomarker, Biosens. Bioelectron. 121 (2018) 243–249.
[60] R. Ramachandran, C. Zhao, M. Rajkumar, K. Krishnamoorthy, P. Zhu, W. Xuan, Z.-X. Xu, F. Wang, Porous nickel oxide microsphere and $Ti_3C_2T_x$ hybrid derived from metal-organic framework for battery-type supercapacitor electrode and non-enzymatic H_2O_2 sensor, Electrochim. Acta 322 (2019), 134771.
[61] L. Yang, D. Liu, J. Huang, T. You, Simultaneous determination of dopamine, ascorbic acid and uric acid at electrochemically reduced graphene oxide modified electrode, Sens. Actuators B 193 (2014) 166–172.
[62] D. Kim, S. Lee, Y. Piao, Electrochemical determination of dopamine and acetaminophen using activated graphene-Nafion modified glassy carbon electrode, J. Electroanal. Chem. 794 (2017) 221–228.
[63] R. Nurzulaikha, H.N. Lim, I. Harrison, S.S. Lim, A. Pandikumar, N.M. Huang, S.P. Lim, G.S.H. Thien, N. Yusoff, I. Ibrahim, Graphene/SnO_2 nanocomposite-modified electrode for electrochemical detection of dopamine, Sens. Bio-Sensing Res. 5 (2015) 42–49.
[64] A. Murali, Y.P. Lan, P.K. Sarawat, M.L. Free, Synthesis of CeO_2/reduced graphene oxide nanocomposite for electrochemical determination of ascorbic acid and dopamine and for photocatalytic applications, Mater. Today Chem. 12 (2019) 222–232.
[65] G.T.S. How, A. Pandikumar, H.N. Ming, L.H. Ngee, Highly exposed {001} factes of titanium dioxide modified with reduced graphene oxide for dopamine sensing, Sci. Rep. 4 (2014) 1–8.
[66] R. Chen, Y. Wang, Y. Liu, J. Li, Selective electrochemical detection of dopamine using nitrogen-doped graphene/manganese monoxide composites, RSC Adv. 5 (2015) 85065–85072.
[67] S. Li, S. Yang, Y. Wang, C. Lien, H. Tien, S. Hsiao, W. Liao, H. Tsai, C. Chang, C. Ma, C. Hu, Controllable synthesis of nitrogen-doped graphene and its effect on the simultaneous electrochemical determination of ascorbic acid, dopamine and uric acid, Carbon 59 (2013) 418–429.
[68] B. Kaur, T. Pandiyan, B. Satpati, R. Srivastava, Simultaneous and sensitive determination of ascorbic acid, dopamine, uric acid, and tryptophan with silver nanoparticles-decorated reduced graphene oxide modified electrode, Colloids Surf. B 111 (2013) 97–106.
[69] V. Mani, R. Devasenathipathy, S.-M. Chen, K. Kohilarani, R. Ramachandran, A sensitive amperometric sensor for the determination of dopamine at graphene and bismuth nanocomposite film modified electrode, Int. J. Electrochem. Sci. 10 (2015) 1199–1207.
[70] A. Rahim, B.A. Barros, L.T. Kubota, Y. Gushikem, SiO_2/C/Cu(II) phthalocyanine as a biometric catalyst for dopamine monooxygenase in the development of an amperometric sensor, Electrochim. Acta 56 (2011) 10116–10121.
[71] Y. Zhang, Z. Xia, H. Liu, M. Yang, L. Lin, Q. Li, Hemin-graphene oxide-pristine carbon nanotubes complexes with intrinsic peroxidase-like activity for the detection of H_2O_2 and simultaneous determination for Trp, AA, DA, and UA, Sens. Actuators B 188 (2013) 496–501.
[72] Y. Wang, Y. Li, L. Tang, J. Lu, J. Li, Application of graphene-modified electrode for selective detection of dopamine, Electrochem. Commun. 11 (2009) 889–892.

Please cite this article as: R. Ramachandran, X. Leng, C. Zhao, et al., 2D siloxene sheets: A novel electrochemical sensor for selective dopamine detection, Appl. Mater. Today, https://doi.org/10.1016/j.apmt.2019.100477